Supplementary Information for "A Shortcut to Garnet-type Fast Li-Ion Conductors for All Solid State Batteries"

By *Semih Afyon*[a], Frank Krumeich[b], and Jennifer L. M. Rupp*[a]*

Supplementary Table 1. Indexed Powder XRD of c-$Li_{6.4}Ga_{0.2}La_3Zr_2O_{12}$ (obtained at 650 °C) using Werner's algorithm (TREOR).

Wavelength : 1.540598

Number of accepted peaks : 36

Crystal system : Cubic or lower
Maximum cell edge : 15.0
Maximum cell volume : 3000.0
2Theta window : 0.050

Maximum unindexed lines for refinement : 0
Required Figure of Merit : 5.0

Selected solution

Symmetry	a	b	c	Volume	FOM	unindexed
Cubic	12.9744	12.9744	12.9744	2184.0	16.9	0

Peak list

N	2Th(obs)	H	K	L	2Th(calc)	obs-calc	Int	d(obs)	d(calc)
1	16.7250	2	1	1	16.7241	0.00089	85.8	5.29650	5.29678
2	19.3405	2	2	0	19.3345	0.00604	14.8	4.58572	4.58714
3	25.6789	3	2	1	25.6701	0.00884	64.9	3.46638	3.46756
4	27.4845	4	0	0	27.4760	0.00848	53.0	3.24262	3.24360
5	30.8062	4	2	0	30.7950	0.01124	100.0	2.90013	2.90117
6	32.3536	3	3	2	32.3382	0.01541	8.4	2.76487	2.76615
7	33.8310	4	2	2	33.8184	0.01262	81.2	2.64743	2.64839
8	35.2579	5	1	0	35.2436	0.01434	6.2	2.54348	2.54449
9	37.9675	5	2	1	37.9538	0.01375	46.5	2.36796	2.36879
10	42.9502	6	1	1	42.9365	0.01373	43.2	2.10408	2.10473
11	44.1170	6	2	0	44.1096	0.00742	6.3	2.05111	2.05143
12	47.5029	6	3	1	47.4906	0.01232	9.0	1.91250	1.91297
13	48.5927	4	4	4	48.5771	0.01563	9.2	1.87213	1.87269
14	50.7096	6	4	0	50.6976	0.01197	31.2	1.79883	1.79923
15	51.7437	5	5	2	51.7340	0.00971	20.2	1.76528	1.76559
16	52.7655	6	4	2	52.7558	0.00974	58.6	1.73348	1.73378
17	55.7524	7	3	2	55.7423	0.01006	11.8	1.64748	1.64775
18	56.7220	8	0	0	56.7142	0.00782	14.9	1.62160	1.62180
19	59.5832	6	5	3	59.5679	0.01533	4.8	1.55038	1.55074
20	60.5251	8	2	2	60.5004	0.02473	2.3	1.52848	1.52905
21	63.2570	7	5	2	63.2487	0.00834	3.6	1.46889	1.46906
22	64.1536	8	4	0	64.1498	0.00381	13.3	1.45051	1.45058
23	65.9340	8	4	2	65.9320	0.00201	14.1	1.41559	1.41562
24	66.8189	7	6	1	66.8137	0.00516	7.1	1.39897	1.39907
25	67.6938	6	6	4	67.6897	0.00407	10.3	1.38300	1.38308
26	68.5505	7	5	4	68.5603	-0.00977	1.7	1.36779	1.36762
27	70.2879	7	6	3	70.2861	0.00179	6.4	1.33818	1.33821
28	72.0068	7	7	0	71.9935	0.01327	1.8	1.31040	1.31061
29	73.6806	7	7	2	73.6846	-0.00396	3.2	1.28472	1.28466
30	77.0164	7	6	5	77.0249	-0.00851	6.5	1.23718	1.23706
31	79.4945	8	6	4	79.5004	-0.00590	10.7	1.20472	1.20464
32	80.3130	10	3	3	80.3209	-0.00793	3.7	1.19449	1.19439
33	81.1261	10	4	2	81.1395	-0.01337	9.6	1.18456	1.18440
34	83.5747	11	2	1	83.5849	-0.01018	5.3	1.15597	1.15585
35	84.3828	8	8	0	84.3972	-0.01439	6.9	1.14694	1.14679
36	86.8126	7	7	6	86.8280	-0.01542	4.2	1.12098	1.12082

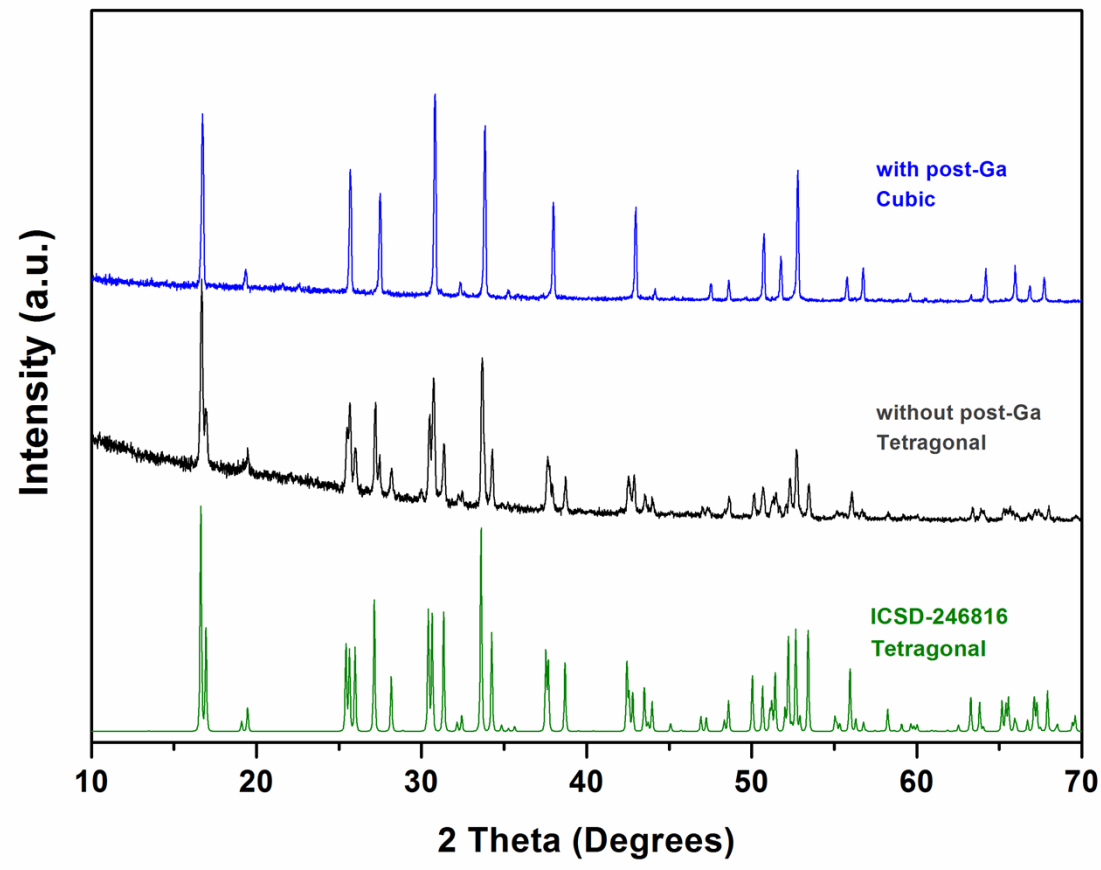

Supplementary Figure S1. XRD powder patterns of the re-annealed $Li_7La_3Zr_2O_{12}$ at 650 °C with (blue) and without (black) post Ga-doping through Ga_2O_3, and the calculated pattern for the tetragonal phase (ICSD 246816).

In order to confirm the influence of post synthetic Ga-doping, already calcined samples are also re-annealed at 650 °C without adding any Ga_2O_3, and in this case, the samples still occurred to be in the tetragonal phase (**Figure S1**).

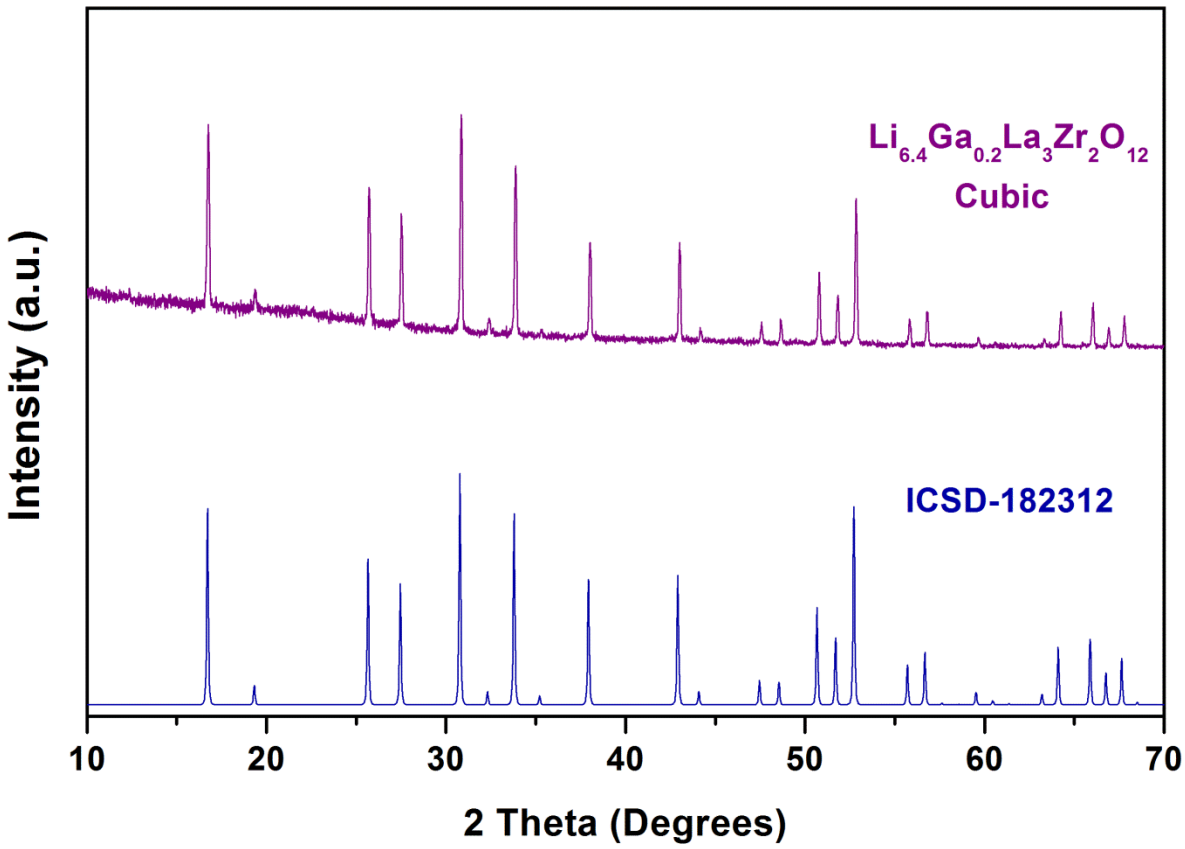

Supplementary Figure S2. XRD powder patterns of c-$Li_{6.4}Ga_{0.2}La_3Zr_2O_{12}$ obtained through post Ga-doping with Ga_2O_3 in glassy carbon crucibles (purple), and the calculated pattern for the cubic phase (ICSD 182312) (blue).

To show that any Al^{3+} contamination through alumina crucibles have no effect on the phase transformation obtained via post Ga-doping with Ga_2O_3, typical syntheses were performed in glassy carbon crucibles rather than alumina crucibles. In a typical synthesis, stoichiometric amounts of Ga_2O_3 and t-$Li_7La_3Zr_2O_{12}$ that would result in a composition of $Li_{6.4}Ga_{0.2}La_3Zr_2O_{12}$ are ground in an agate mortar. Annealing Ga_2O_3 + t-$Li_7La_3Zr_2O_{12}$ mixture at ~ 650-800 ^oC for 10-15 hours under Ar flow in glassy carbon crucibles yields the cubic phase c-$Li_{6.4}Ga_{0.2}La_3Zr_2O_{12}$ (**Figure S2**).

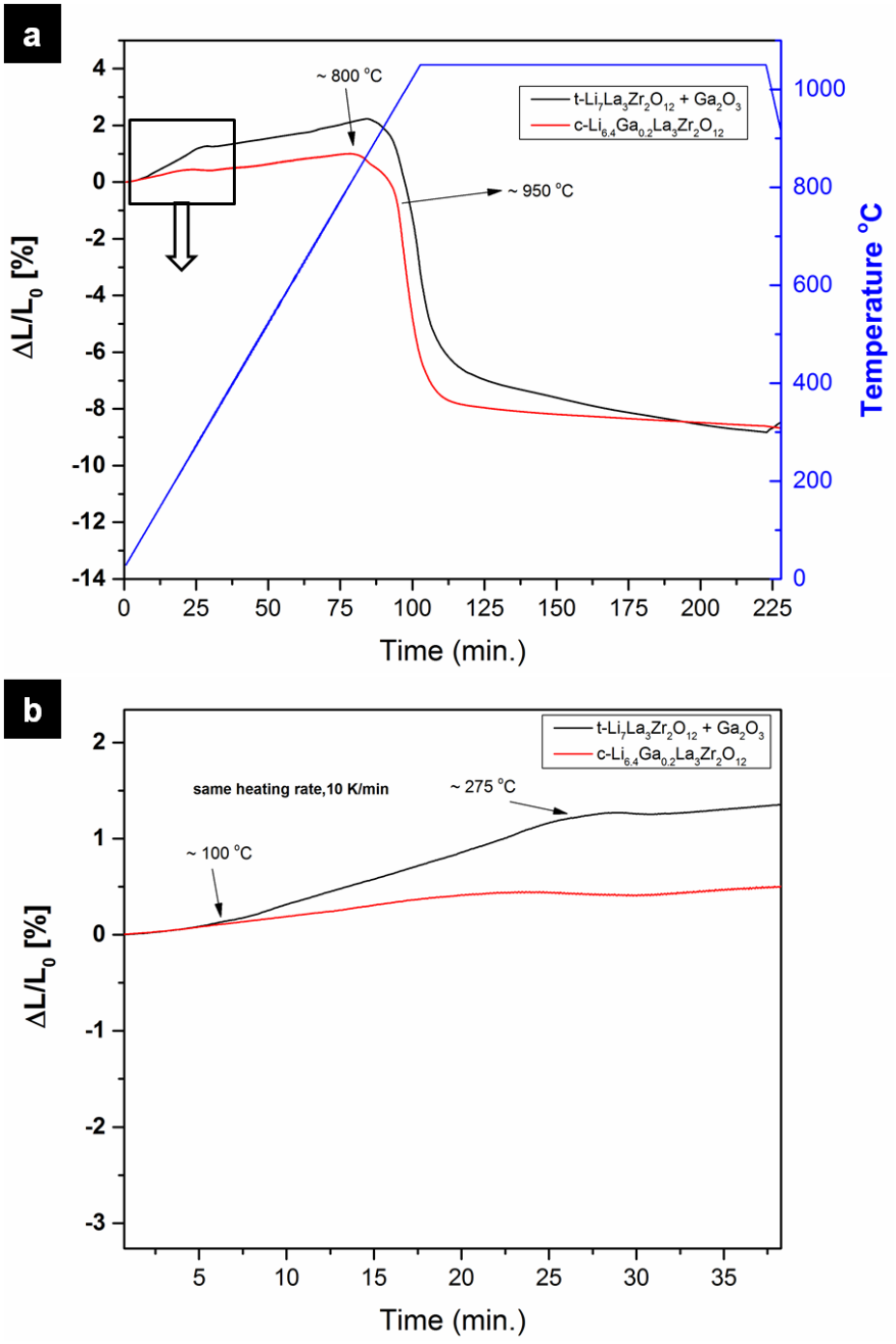

Supplementary Figure S3. a) Dilatometry curves for t-$Li_7La_3Zr_2O_{12}$ + Ga_2O_3 and c-$Li_{6.4}Ga_{0.2}La_3Zr_2O_{12}$ displaying the main sintering phases, at a heating rate of 10 °C / min. **b)** the magnified marked region from Figure S2a**,** comparing the dilatometry curves for t-$Li_7La_3Zr_2O_{12}$ + Ga_2O_3 mixture and c-$Li_{6.4}Ga_{0.2}La_3Zr_2O_{12}$ showing the phase transformation at ~ 100 °C.

Dilatometry curves are displayed for t-$Li_7La_3Zr_2O_{12}$ + Ga_2O_3 and already transformed c-$Li_{6.4}Ga_{0.2}La_3Zr_2O_{12}$ in **Figure S3**. The dilatometry curves confirm the phase transformation at low temperature. A volume expansion starting from ~ 100 ^oC is observable for a pellet of the Ga_2O_3 + t-$Li_7La_3Zr_2O_{12}$ mixture that also manifests itself as a broad peak in differential dilatometry curves (**Fig. 2b** main text), whereas such volume changes are not present for the pellets of t-$Li_7La_3Zr_2O_{12}$ and already transformed c-$Li_{6.4}Ga_{0.2}La_3Zr_2O_{12}$. The onset temperature and the main sintering peak for c-$Li_{6.4}Ga_{0.2}La_3Zr_2O_{12}$ pellets are also found to be ~ 800 ^oC and ~ 950-975 ^oC, respectively, which is 200-300 ^oC lower than the values reported in literature. No sintering can be observed for the tetragonal phase of t-$Li_7La_3Zr_2O_{12}$, and the low ionic conductivities obtained for the tetragonal phase so far could also be linked to this finding.

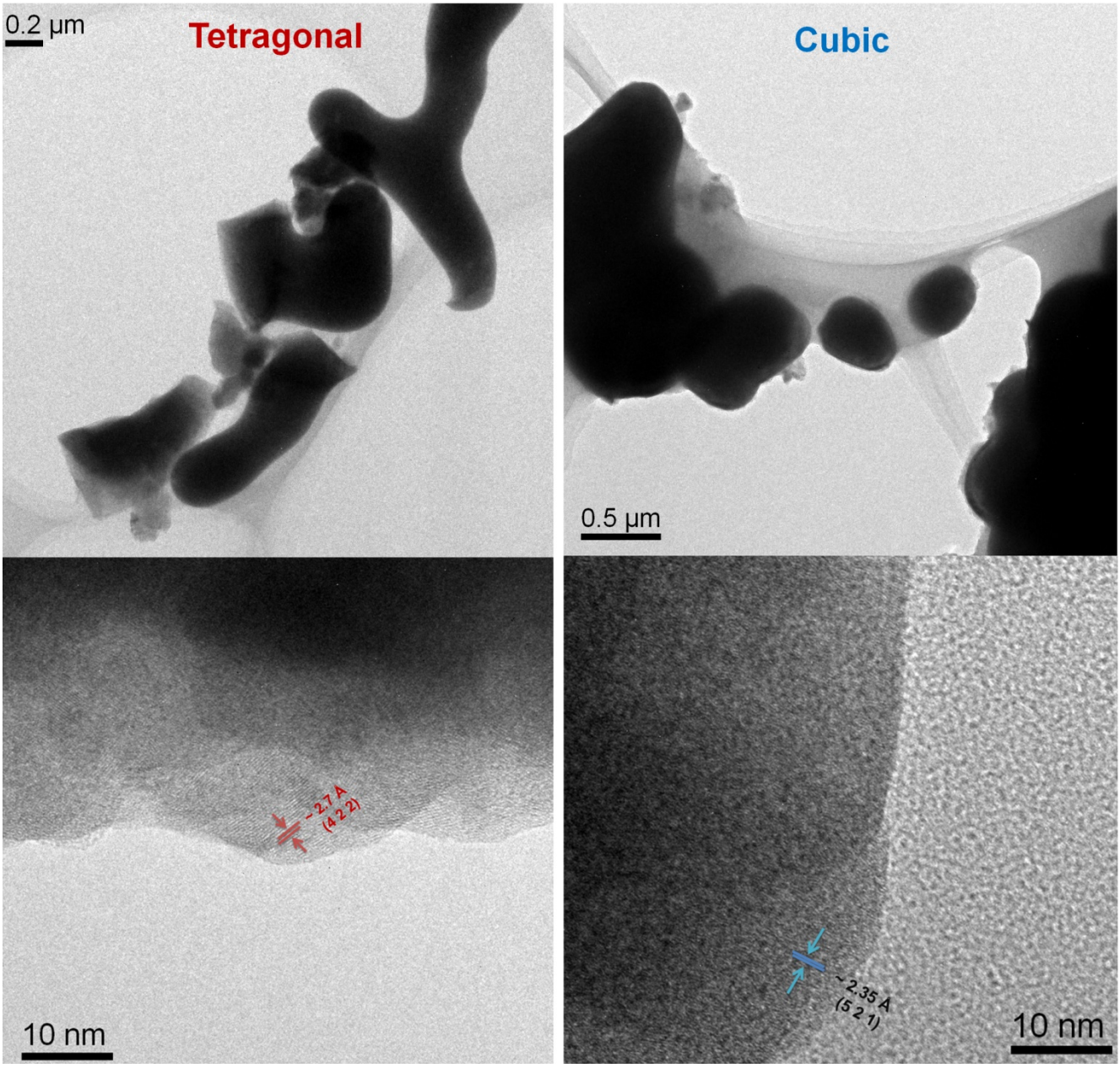

Supplementary Figure S4. Transmission electron microscopy images (TEM) of t-$Li_7La_3Zr_2O_{12}$ (red) and c-$Li_{6.4}Ga_{0.2}La_3Zr_2O_{12}$ (blue).

Transmission electron microscopy images (TEM) of t-$Li_7La_3Zr_2O_{12}$ (red) and c-$Li_{6.4}Ga_{0.2}La_3Zr_2O_{12}$ (blue) are shown in **Figure S4**. t-$Li_7La_3Zr_2O_{12}$ appears as elongated particles in the range of 300 nm to 1 µm with no well-defined shapes. With the phase transformation to the cubic phase, the spherical nano-crystallites of c-$Li_{6.4}Ga_{0.2}La_3Zr_2O_{12}$ that are mostly in the

range of ~ 200 - 300 nm can be observed in TEM images. The lattice fringes corresponding to the marked planes could also be found in high resolution images.

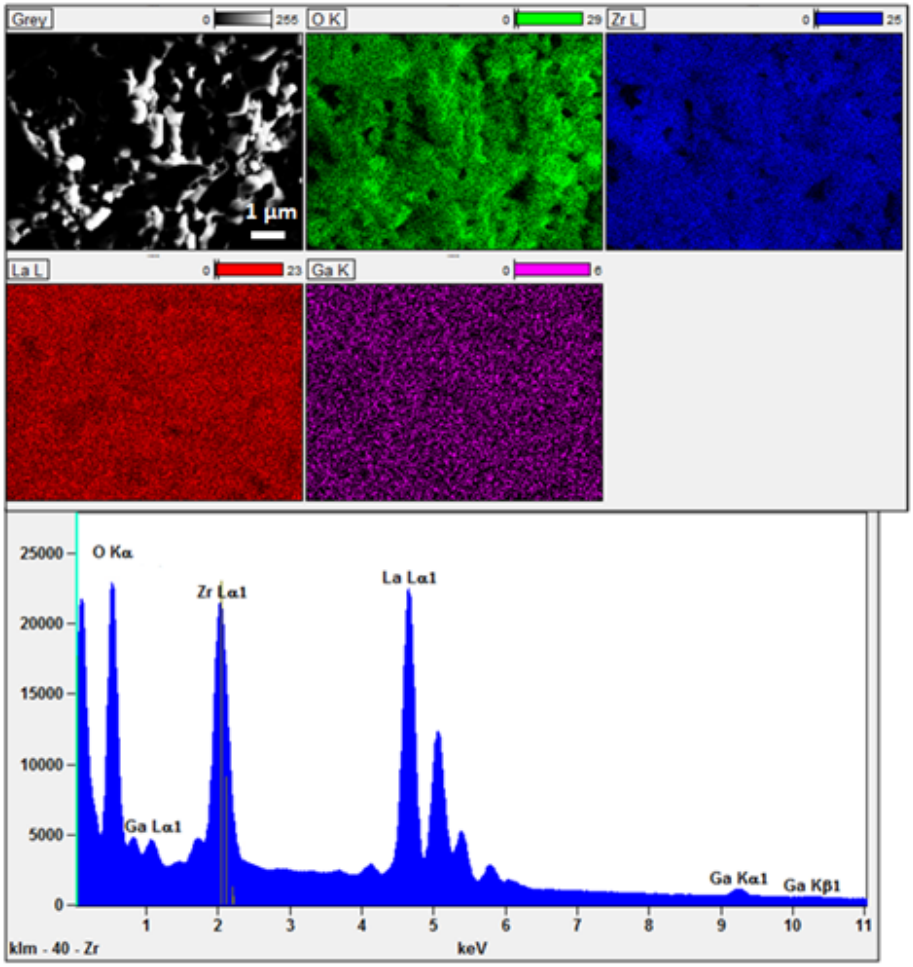

Element Line	Net Counts	Net Error	k-ratio (calc.)	Element wt-%	wt-% error	Theoretical wt-%
O_K	277517	±2001	0.138	24.04	±0.17	23.85
Ga_L	23461	±1120	0.012	2.25	±0.11	1.73
Zr_L	443627	±2597	0.234	23.59	±0.14	22.66
La_L	732578	±3680	0.616	50.12	±0.25	51.76

Supplementary Figure S5. SEM-EDXS analysis of c-$Li_{6.4}Ga_{0.2}La_3Zr_2O_{12}$ pellet cross-sectional surface (sintering at 950 ^oC for 6 hours). Elemental mapping of cubic c-$Li_{6.4}Ga_{0.2}La_3Zr_2O_{12}$ and EDX spectrum from the selected area are presented. The homogeneous distribution of O (green), Zr (blue), La (red) and Ga (purple) are shown. Theoretical elemental ratios given in the table are calculated based on $Li_{6.4}Ga_{0.2}La_3Zr_2O_{12}$ formula.

Figure S5 shows SEM-EDXS analysis performed at c-$Li_{6.4}Ga_{0.2}La_3Zr_2O_{12}$ pellet cross-sectional surface after sintering to 950 ^oC for 6 hours. A homogeneous distribution of elements is also found here, and again, no enrichment neither in the bulk grain cores nor towards the grain boundary-close interfaces are measurable within the limits of the technique and elemental mapping carried out. Besides, a composition in close proximity to the intended initial compound ($Li_{6.4}Ga_{0.2}La_3Zr_2O_{12}$) is found, but, still, we should note that elemental analysis from EDX spectrum should be evaluated in a qualitative basis, so further studies (e.g. ICP-OES) that is the beyond the scope of current work may help to find out the exact composition of processed pellets.

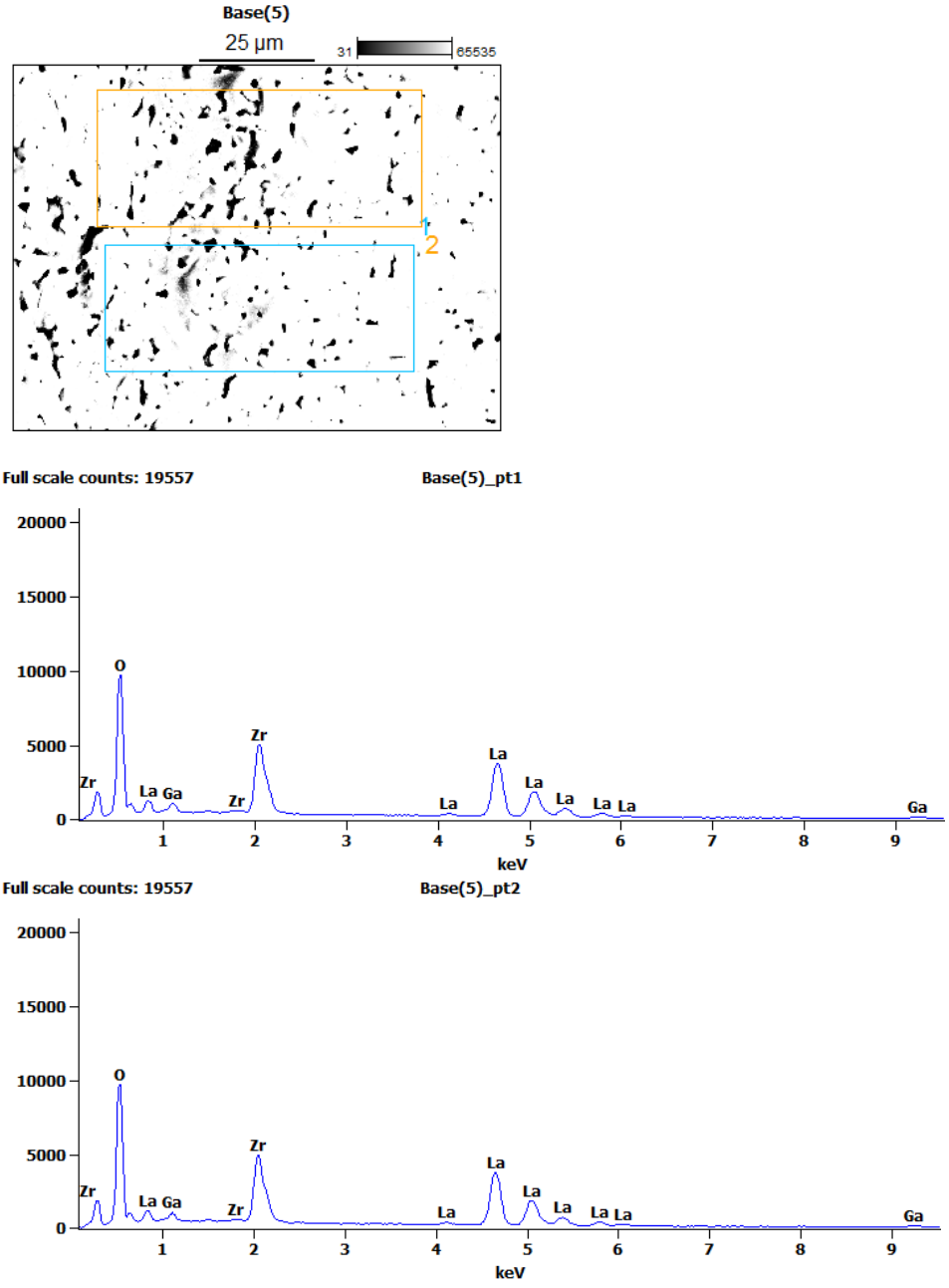

Supplementary Figure S6. EDX analysis of c-$Li_{6.4}Ga_{0.2}La_3Zr_2O_{12}$ pellet cross-sectional surface (sintering at 950 ºC for 6 hours). EDX Spectra acquired from the selected zones in the cross-sectional image don't show any Al contamination that might result from the alumina crucibles used during the sintering of pellets.

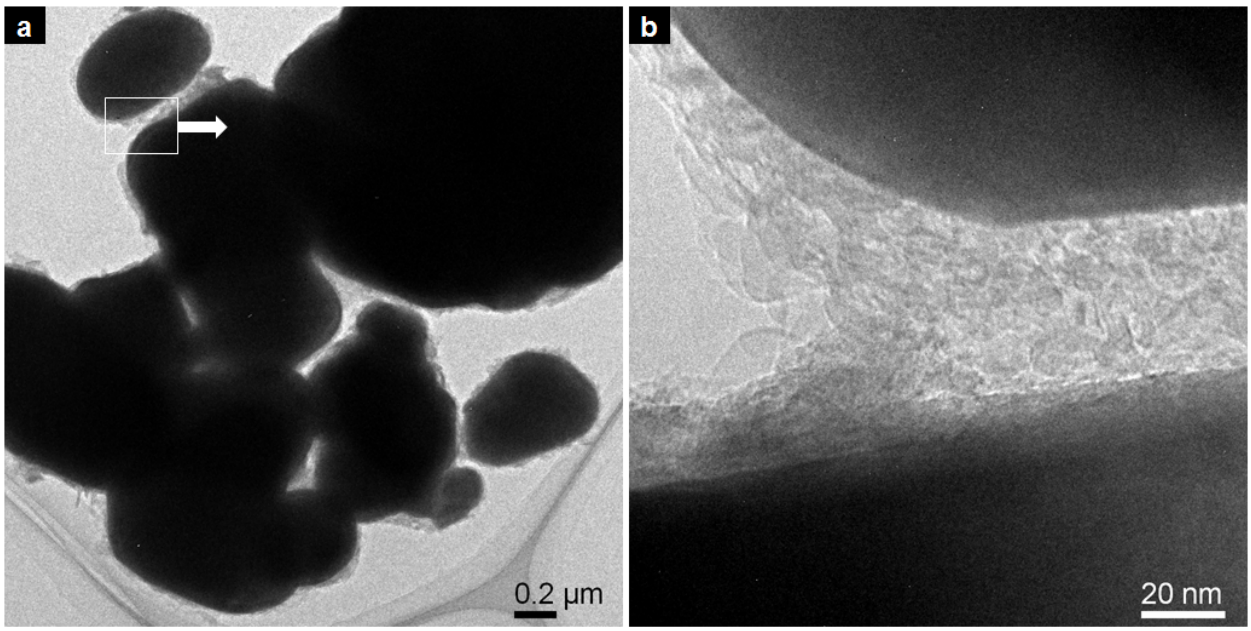

Supplementary Figure S7. a) Transmission electron microscopy image (TEM) of c-$Li_{6.4}Ga_{0.2}La_3Zr_2O_{12}$ showing particle agglomerates, **b)** the magnified marked region from Figure S5a displaying amorphous inter-granular phases between c-$Li_{6.4}Ga_{0.2}La_3Zr_2O_{12}$ nano-particles.

The presence of amorphous inter-granular phases is shown **Figure S7b**, where the amorphous nano-particles with a lack of order even at 20 nm resolution can be observed. The exact nature of these inter-granular phases couldn't be revealed here, as we were not able to perform HRTEM and SAED from the selected areas due to the instability of particles under e-beam. Nevertheless, the direct evidence of amorphous inter-granular is revealed, and unreacted Ga_2O_3, Li-compounds (e.g. Li_2O, Li_2CO_3) that could eventually form in air starting from the exchange of Li^+ in LLZO structure with Ga^{3+}, $LiGaO_2$ and other glassy Ga and Li rich materials could be speculated as the constituents of inter-granular phase

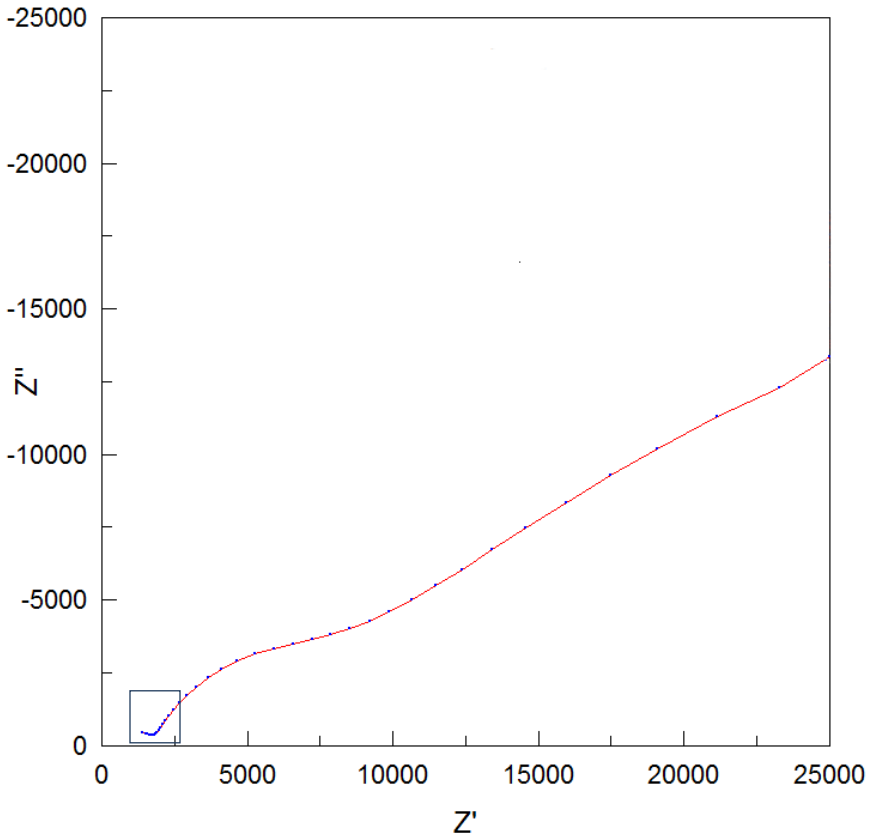

Supplementary Figure S8. Nyquist plot obtained from a pellet of c-$Li_{6.4}Ga_{0.2}La_3Zr_2O_{12,}$ exposed to air for ~ 2-3 hours (after the production of the measurement pellet with electrodes) at RT ^{o}C in air using Pt electrodes (1 MHz to 1 Hz).

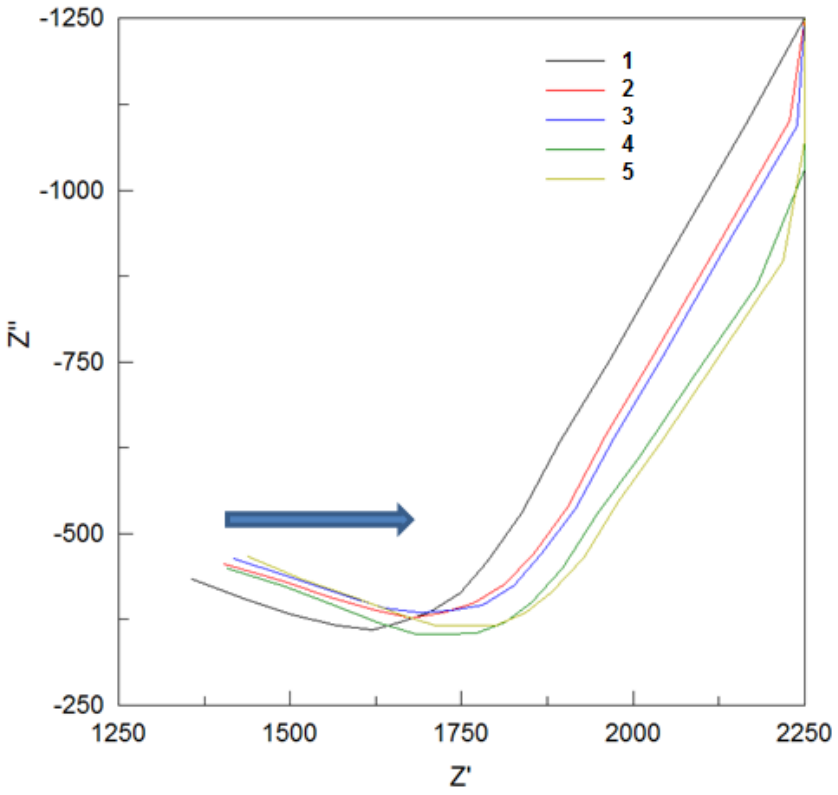

Supplementary Figure S9. Consecutive measurements in ~ 10 minutes intervals from the c-$Li_{6.4}Ga_{0.2}La_3Zr_2O_{12}$ pellet in Figure S4 displaying the increase in resistance with prolonged air exposure (magnified region in Fig. S4 is shown for consecutively obtained Nyquist plots)

After the production of a pellet of c-$Li_{6.4}Ga_{0.2}La_3Zr_2O_{12}$ for AC measurements, it was exposed to air for ~ 2-3 hours. The Nyquist plot obtained from such a pellet at RT ^{o}C in air using Pt electrodes (1 MHz to 1Hz) is displayed in **Figure S8**. The bulk contribution becomes more apparent with an incomplete semicircle at high frequency for the higher resistive pellet (**Fig. S8**). Consecutive impedance spectra measured from the same pellet with 10 minutes of waiting periods in air are displayed in **Figure S9**. The bulk resistance increases as the pellets are exposed to air for longer period of times that is consistent with the negative effect of humidity on the conductivity that was reported before.

Supplementary Table 2. Indexed Powder XRD of c-$Li_{6.4}Ga_{0.2}La_3Zr_2O_{12}$ pellet material (sintered at 950°C) using Werner's algorithm (TREOR).

Wavelength : 1.540598

Number of accepted peaks : 25

Crystal system : Cubic or lower
Maximum cell edge : 15.0
Maximum cell volume : 3000.0
2Theta window : 0.050

Maximum unindexed lines for refinement : 1
Required Figure of Merit : 5.0

Selected solution

Symmetry	a	b	c	Volume	FOM	unindexed
Cubic	12.9706	12.9706	12.9706	2182.1	25.2	0

Peak list

N	2Th(obs)	H	K	L	2Th(calc)	obs-calc	Int	d(obs)	d(calc)
1	16.7194	2	1	1	16.7291	-0.00968	67.3	5.29827	5.29522
2	19.3129	2	2	0	19.3402	-0.02732	16.0	4.59223	4.58579
3	25.6682	3	2	1	25.6778	-0.00957	50.2	3.46780	3.46653
4	27.4782	4	0	0	27.4843	-0.00609	46.3	3.24335	3.24264
5	30.8096	4	2	0	30.8043	0.00533	100.0	2.89982	2.90031
6	32.3242	3	3	2	32.3480	-0.02379	8.9	2.76732	2.76534
7	33.8110	4	2	2	33.8287	-0.01765	73.2	2.64895	2.64761
8	35.2300	5	1	0	35.2543	-0.02429	7.9	2.54544	2.54374
9	37.9639	5	2	1	37.9654	-0.00147	43.8	2.36818	2.36809
10	42.9382	5	3	2	42.9498	-0.01156	38.4	2.10465	2.10411
11	44.1003	6	2	0	44.1233	-0.02298	5.9	2.05184	2.05083
12	47.5050	6	3	1	47.5055	-0.00045	9.0	1.91243	1.91241
13	48.5899	4	4	4	48.5923	-0.00243	9.9	1.87223	1.87214
14	50.7190	6	4	0	50.7136	0.00536	36.1	1.79852	1.79870
15	51.7540	5	5	2	51.7504	0.00363	20.1	1.76496	1.76507
16	52.7630	6	4	2	52.7725	-0.00953	63.0	1.73356	1.73327
17	55.7766	7	3	2	55.7602	0.01638	11.5	1.64682	1.64727
18	56.7336	8	0	0	56.7324	0.00117	17.8	1.62129	1.62132
19	59.5734	6	5	3	59.5872	-0.01382	4.4	1.55061	1.55028
20	64.1603	8	4	0	64.1710	-0.01067	14.9	1.45037	1.45015
21	65.9651	8	4	2	65.9539	0.01120	20.3	1.41499	1.41521
22	66.8492	7	6	1	66.8360	0.01315	8.5	1.39841	1.39865
23	67.7022	6	6	4	67.7124	-0.01020	14.1	1.38285	1.38267
24	70.3216	7	6	3	70.3099	0.01169	7.3	1.33762	1.33781
25	73.7175	7	7	2	73.7099	0.00761	4.1	1.28417	1.28428

Supplementary Table 3. Indexed Powder XRD of c-$Li_{6.4}Ga_{0.2}La_3Zr_2O_{12}$ pellet material (sintered at 1100°C) using Werner's algorithm (TREOR).

Wavelength : 1.540598

Number of accepted peaks : 25

Crystal system : Cubic or lower
Maximum cell edge : 15.0
Maximum cell volume : 3000.0
2Theta window : 0.050

Maximum unindexed lines for refinement : 1
Required Figure of Merit : 5.0

Selected solution

Symmetry	a	b	c	Volume	FOM	unindexed
Cubic	12.9584	12.9584	12.9584	2176.0	20.6	1

Peak list

N	2Th(obs)	H	K	L	2Th(calc)	obs-calc	Int	d(obs)	d(calc)
1	16.7440	2	1	1	16.7449	-0.00092	100.0	5.29053	5.29024
2	19.3478	2	2	0	19.3586	-0.01078	15.7	4.58402	4.58148
3	23.6396			Peak not indexed			8.2	3.76059	
4	25.7019	3	2	1	25.7023	-0.00042	69.1	3.46334	3.46328
5	27.4735	4	0	0	27.5106	-0.03714	40.7	3.24389	3.23960
6	30.8324	4	2	0	30.8339	-0.00155	75.8	2.89773	2.89759
7	32.3732	3	3	2	32.3792	-0.00604	8.8	2.76324	2.76274
8	33.8746	4	2	2	33.8614	0.01318	76.9	2.64412	2.64512
9	38.0144	5	2	1	38.0024	0.01196	38.7	2.36515	2.36587
10	43.0014	6	1	1	42.9922	0.00925	35.2	2.10170	2.10213
11	47.5537	6	3	1	47.5529	0.00083	7.8	1.91058	1.91061
12	48.6408	4	4	4	48.6410	-0.00017	10.1	1.87039	1.87038
13	50.7647	6	4	0	50.7647	-0.00000	27.3	1.79701	1.79701
14	51.8048	5	5	2	51.8026	0.00216	17.3	1.76335	1.76341
15	52.8349	6	4	2	52.8260	0.00891	53.2	1.73137	1.73164
16	55.7936	7	3	2	55.8172	-0.02362	10.4	1.64636	1.64572
17	56.7805	8	0	0	56.7906	-0.01011	9.5	1.62006	1.61980
18	59.6635	6	5	3	59.6489	0.01459	5.1	1.54848	1.54882
19	64.1908	8	4	0	64.2385	-0.04774	15.4	1.44975	1.44879
20	66.0193	8	4	2	66.0238	-0.00452	12.4	1.41396	1.41388
21	66.9037	7	6	1	66.9072	-0.00345	7.0	1.39740	1.39734
22	67.7856	6	6	4	67.7847	0.00089	13.8	1.38135	1.38137
23	70.4101	7	6	3	70.3858	0.02429	6.8	1.33616	1.33656
24	77.1722	7	6	5	77.1376	0.03458	6.2	1.23507	1.23553
25	79.6028	10	4	0	79.6182	-0.01539	9.2	1.20335	1.20316